APL Photonics

RESEARCH ARTICLE | AUGUST 30 2022

High bandwidth frequency modulation of an external cavity diode laser using an intracavity lithium niobate electro-optic modulator as output coupler

S. Palmer ; A. Boes ; G. Ren ; T. G. Nguyen ; S. J. Tempone-Wiltshire; N. Longhurst; P. M. Farrell ; A. Steiner ; Ch. D. Marciniak ; T. Monz ; A. Mitchell ; R. E. Scholten

Check for updates

APL Photonics 7, 086106 (2022)
https://doi.org/10.1063/5.0097880
CHORUS

View Online
Export Citation
CrossMark

10 November 2023 04:28:51

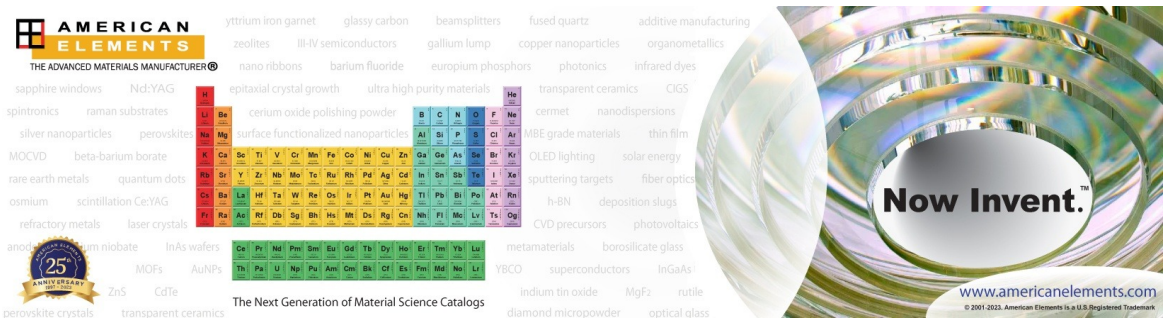

AIP Publishing

High bandwidth frequency modulation of an external cavity diode laser using an intracavity lithium niobate electro-optic modulator as output coupler

Cite as: APL Photon. 7, 086106 (2022); doi: 10.1063/5.0097880
Submitted: 3 May 2022 • Accepted: 29 July 2022 •
Published Online: 30 August 2022

View Online Export Citation CrossMark

S. Palmer,[1,a)] A. Boes,[1] G. Ren,[1] T. G. Nguyen,[1] S. J. Tempone-Wiltshire,[2] N. Longhurst,[2] P. M. Farrell,[2] A. Steiner,[3] Ch. D. Marciniak,[3] T. Monz,[3,4] A. Mitchell,[1] and R. E. Scholten[2,5]

AFFILIATIONS

[1] Integrated Photonics and Applications Centre (InPAC), School of Engineering, RMIT University, Melbourne 3000, Australia
[2] MOGLabs, Carlton 3053, Australia
[3] Institut für Experimentalphysik, 6020 Innsbruck, Austria
[4] Alpine Quantum Technologies (AQT), 6020 Innsbruck, Austria
[5] School of Physics, University of Melbourne, Parkville 3010, Australia

[a)] **Author to whom correspondence should be addressed:** sonya.palmer@student.rmit.edu.au

ABSTRACT

We present a novel approach to high bandwidth laser frequency modulation. A lithium niobate chip is used as an intracavity electro-optic modulator in a tunable cateye external cavity diode laser. The modulator is conveniently integrated with the cateye output coupler, providing a unique approach to high bandwidth frequency stabilization and linewidth narrowing. The intracavity modulator feedback was successfully operated below 1 V and achieved superior frequency noise suppression compared to conventional feedback through diode injection current modulation. A closed loop bandwidth of 1.8 MHz was demonstrated, and the laser linewidth reduced to around 1 Hz as measured by the heterodyne measurement.

© 2022 Author(s). All article content, except where otherwise noted, is licensed under a Creative Commons Attribution (CC BY) license (http://creativecommons.org/licenses/by/4.0/). https://doi.org/10.1063/5.0097880

INTRODUCTION

Narrow linewidth frequency stabilized lasers are the basis of a wide range of applications from spectroscopy[1] and metrology[2] to precision timekeeping,[3] atom trapping and cooling,[4] and ion and atom qubits for quantum computation.[5] External cavity semiconductor diode lasers (ECDLs) are predominantly used for such applications owing to their small size and weight, high efficiency, low cost, diverse wavelength coverage, tunability, low intensity noise, and narrow frequency linewidth. While the achievable linewidth and stability of these lasers are effective for many applications, advances in precision timekeeping[6,7] quantum sensing,[8] and quantum computing[9] continue to further push the requirements for narrower linewidth and faster frequency control.

Frequency stabilization of ECDLs by using the feedback signal from comparison to a second reference laser, an atomic vapor cell, or a high-finesse cavity can be used to actively reduce the laser frequency uncertainty and linewidth. The feedback error signal drives one or more frequency actuators in the laser, typically a piezoelectric transducer for slow changes with a large laser frequency tuning range, and the diode injection current for smaller but faster corrections of the lasing frequency. The diode current response is a combination of relatively slow thermal effects and much faster refractive index changes related to the carrier density in the semiconductor gain medium,[10] and will lead to an increase in the laser's relative intensity noise (RIN). Ideally, the active feedback linewidth reduction requires a feedback bandwidth that is comparable to, or greater than, the technical noise broadened ECDL

10 November 2023 04:28:51

linewidth. In practice, it is challenging to achieve a feedback bandwidth of 2–3 MHz needed for sub-Hz linewidth by using this approach.

Intracavity electro-optic phase modulators (EOMs) offer an attractive alternative as a frequency feedback actuator.[11–16] EOMs can have high bandwidth with a flat frequency response, from DC to many megahertz and even gigahertz with greatly reduced RIN when compared to modulating the laser diode current. For practical implementation in a laser cavity, a large crystalline EOM is typically used, for example, on the order of $4 \times 10 \times 40$ mm^3.[14] Large crystals are required to accommodate the 1–2 mm laser beam diameter in the cavity. The thickness of the crystal also reduces the electric field when applying a voltage to the electrodes, and therefore, relatively long crystals are needed to increase the electro-optic interaction length and reduce the driving voltage needed for a given phase shift.

In this paper, we experimentally demonstrate an EOM for intra-cavity linewidth narrowing, which is very compact and easily integrated into a cateye laser cavity configuration.[17] A custom-made lithium niobate modulator is positioned at the focus of the cateye lens such that the active area of the modulator is small, enabling small electrode separation and, thus, a high field strength for a given electric potential difference. That, in turn, allows for a very short crystal interaction length, as short as the thickness of standard lithium niobate ($LiNbO_3$, LN) wafers (0.5 mm in our case), and fabrication using standard wafer processing methods. The compact size results in small capacitance and high modulation bandwidth. We demonstrate our intracavity EOM by using the Pound–Drever–Hall (PDH) technique for locking and linewidth narrowing of a 729 nm wavelength laser (the wavelength of the optical clock transition of $^{40}Ca^+$) to a high-finesse cavity. The intracavity modulator allows greater frequency noise suppression over a wider bandwidth compared to feedback via conventional modulation of the diode injection current.

BACKGROUND

Figure 1(a) shows the configuration of a standard cateye ECDL,[17] with a large bulk electro-optic modulator (EOM) within the cavity. The cateye cavity configuration[17] is self-aligning and, thus, mechanically robust and also ensures high efficiency of coupling between the diode and the external cavity, which reduces the linewidth. The cateye ECDL cavity length is typically around 30 mm with a 5 GHz free spectral range (FSR). An ultranarrow bandpass filter (bandwidth 0.20 ± 0.03 nm) is used to select a single external cavity mode. The rotation of the filter allows for tuning over a range of tens of nanometers, without affecting the direction of the output beam. The output coupler optic is fixed to a piezoelectric transducer that allows adjustment of the external cavity length and, thus, laser frequency over tens of GHz, with a bandwidth of tens of kHz. The EOM introduced here provides fast, high-fidelity control required for qubit manipulation, and linewidth narrowing needed for sensing and clock applications.

Figure 1(b) shows the design of the EOM output coupler, which uses an LN chip, with a thickness of 0.5 mm and a length and width of 4.2 mm. The chips were fabricated from a 76 mm X-cut Magnesium doped LN wafer. Magnesium doped wafers were used as they

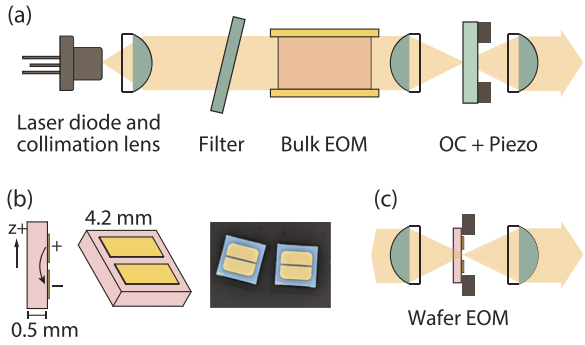

FIG. 1. (a) Schematic of cateye external cavity laser[17] showing placement of an intra-cavity bulk crystal electro-optic modulator. OC: output coupler. (b) Schematic and photograph of wafer-based lithium niobate intra-cavity modulator with rectangular gold electrodes of 100 nm thickness. The gap spacing of the electrodes varied from 0.1 to 0.5 mm. An arrow between the electrodes indicates the electric field between them. (c) Modified cateye external cavity laser configuration with LN intra-cavity modulator. The inside surface is antireflection (AR) coated for 729 nm; the exit surface is uncoated, with Fresnel reflectivity of 15%.

are more robust to optical damage and degradation of the electro-optic effect when used at high optical power. After the deposition and patterning of 100 nm thick gold electrodes on the exit surface of the EOM, an antireflection (AR) coating for a wavelength of 729 nm was applied on the opposite surface. Figure 1(c) shows how the EOM acts as a partial mirror, replacing the fused silica of a typical cateye cavity output coupler. The cavity is formed between the laser diode highly reflecting rear facet and the reflectivity of the uncoated exit surface of the EOM, which has a Fresnel reflectivity of 15%, for a wavelength of 729 nm. A potential difference between the electrodes establishes an electric field that has a strong field component along LN's crystallographic z axis and is perpendicular to the laser propagation axis. If the polarization of the laser light is also along LN's crystallographic z axis, then the r_{33} electro-optic tensor element is the dominant electro-optic effect on the refractive index within the crystal.

The electro-optic coefficient $r_{33} = 32$ pm/V is small, and therefore, to achieve high phase modulation at practical electric potential differences, conventional single-crystal modulators (which are designed to work outside a laser cavity) are typically 20 or 30 mm in length and operate at hundreds of volts to achieve a few radians of phase shift. Our wafer-fabricated device relies on enhancement within a laser cavity, such that a 0.5 mm crystal can operate effectively at just a few volts. The change in frequency df due to refractive index change in the EOM is

$$\mathrm{d}f = \frac{f_0 dL}{L},$$

where $f_0 = c/\lambda_0$, c is the speed of light in vacuum, and λ_0 is the unmodulated wavelength, determined by the laser diode and filter angle (in our case, $\lambda_0 = 729$ nm). L is the cavity length, and the change in cavity length due to change in refractive index is $dL = L_{\mathrm{LN}}\mathrm{d}n$, where L_{LN} is the thickness of the LN wafer and dn is

$$\mathrm{d}n = \frac{1}{2} r_{33} n^3 E,$$

10 November 2023 04:28:51

© Author(s) 2022

with $n = 2.2022$ being the extraordinary refractive index of LN at 729 nm.

We used finite element analysis (CST Studio Suite®) to calculate the field strength in two dimensions through the thickness of the substrate with electrode separation of 0.3 mm and a potential difference of 1 V. Figure 2(a) shows a cross-section of the z-component of the field strength between the electrodes, and Fig. 2(b) shows the field strength of the z-component along the x axis (propagation direction) with the shaded region showing the field strength within the LN substrate. The calculated change in refractive index is $dn = 4.2 \times 10^{-11}$.

We investigated electrodes with a range of gap spacings (d_{gap}), from 0.1 to 0.5 mm. For a given potential difference, a smaller gap creates a stronger field, but increases the capacitance and reduces the bandwidth. For our devices, the capacitance of the electrode pair was below 0.1 pF even for the smallest gap, and, in practice, is overwhelmed by parasitic capacitance in the electrical connections and driving circuit. Hence, smaller gaps would be preferable; however, a smaller gap requires more accurate alignment to the laser axis and cateye focus. The spot-size of the beam at the cateye focus is ~1.2 μm ($1/e^2$ diameter), with displacement around 0.1 mm per degree of incident angle. To accommodate imperfect alignment, an electrode spacing of 0.3 mm was chosen, giving an estimated frequency shift for 30 mm cavity length, 0.5 mm LN wafer, and 729 nm laser as

$$df = f_0 \frac{L_{LN}}{L} dn = \frac{c}{\lambda_0} \frac{L_{LN}}{L} 4.15 \times 10^{-11} \frac{V}{d_{gap}} = 0.9 \text{ MHz/V}.$$

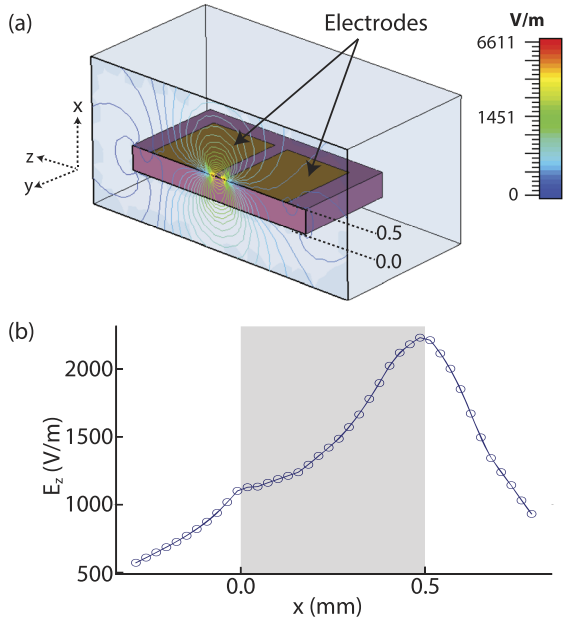

FIG. 2. Calculated electric field in the LN wafer modulator. (a) Cross-section of the E_z component of the field strength between the electrodes of the modulator. (b) E_z component of field strength along the x-direction with the area of the LN modulator indicated by the shaded region of the plot.

In other words, a potential difference of 1 V will shift the cavity lasing frequency by 0.9 MHz, approximately ten times greater than the passive linewidth of an ECDL. Therefore, in active corrections for frequency fluctuations of the laser and reduction of the effective linewidth, our wafer-fabricated cateye modulator will theoretically operate at the output voltages of common low-voltage op-amp circuits. We have also successfully used the modulators at up to 20 Vpp.

INTRA-CAVITY ELECTRO-OPTIC MODULATOR SENSITIVITY AND BANDWIDTH

We used a high-finesse optical cavity to measure the spectral output of the cateye ECDL. The laser frequency was scanned across the cavity resonance (cavity linewidth 70 kHz) while driving the intra-cavity EOM with a sinusoidal modulation at varying frequency. The electric field of the modulated laser output is proportional to $\cos(2\pi f_0 t + \beta \sin(2\pi f_m t)) = \sum_n J_n(\beta) \cos(2\pi(f_0 + n f_m)t)$, where f_0 and f_m are the carrier and modulation frequencies, respectively, and $J_n(\beta)$ is the Bessel function, with $\beta = \Delta f / f_m$ being the modulation index, that is, the maximum frequency deviation in terms of the modulation frequency. We fit the square of the electric field to the measured power spectrum, varying β to best match the relative power in each of the peaks, which are proportional to J_n^2. The sensitivity is then $\Delta f / V$, where $\Delta f = \beta f_m$ and V is the amplitude of the sinusoid driving the modulator. Figure 3(b) shows the measured sensitivity varying from 0.6 to 1.4 MHz/V over a range of frequencies from DC to 16 MHz, consistent with the 0.9 MHz/V calculated earlier. At higher modulation frequency, the sideband amplitudes become too small to measure with this approach. Instead, we locked the laser frequency to the cavity by using diode current feedback (see later) and used a signal generator to drive the intra-cavity modulator. We measured the response of the error signal for varying modulation frequency, relative to the $1/f_{mod}$ decrease expected for the locking error signal.[18] The 8 dB decrease over 50 MHz is consistent with the loss expected for an unterminated coax: the modulator is connected via coax and then ~10 cm of untwisted pair 32 AWG wire. The measured loss is very similar to the loss for the cable and untwisted wire without modulator, as measured using a vector network analyzer.

INTRA-CAVITY ELECTRO-OPTIC MODULATOR LINEWIDTH NARROWING

To demonstrate the effectiveness of the intracavity modulator, we used Pound–Drever–Hall (PDH) locking[19] of the laser to a high-finesse cavity [see Fig. 4(a)]. Frequency modulation at ±20 MHz was added with a fiber-coupled electro-optic phase modulator (ixBlue NIR-MPX800-LN-0.1). The reference cavity had a finesse of 21 000, a linewidth of 70 kHz, and free spectral range of 1.5 GHz. The light reflected from the cavity was detected with an amplified photodiode (Thorlabs PDA10A-EC) and mixed with the 20 MHz local oscillator to create a PDH error signal. The error signal was filtered by using a high-bandwidth low-latency servo controller (MOGLabs FSC). The low-frequency (SLOW) output from the fast servo controller (FSC) was connected to the laser piezo driver to correct for slow

10 November 2023 04:28:51

© Author(s) 2022

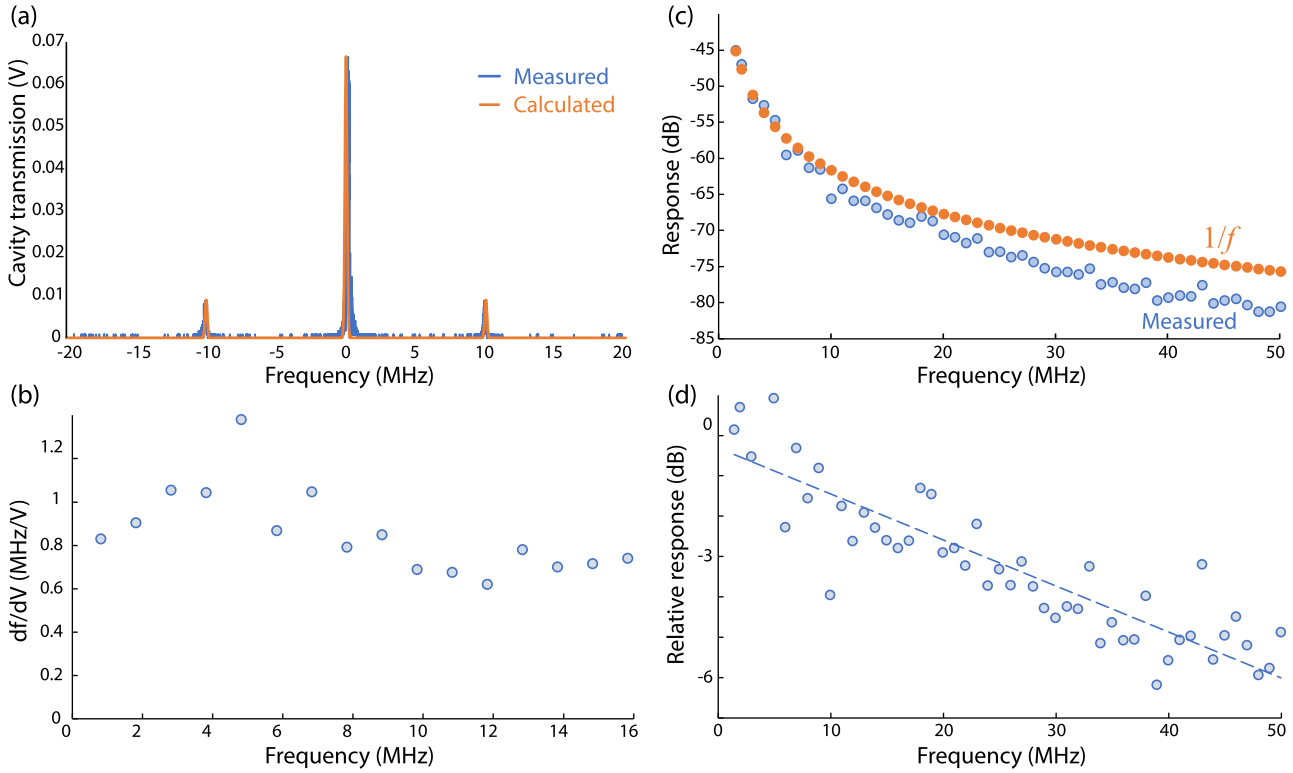

FIG. 3. (a) Laser spectrum at modulation frequency 10 MHz, measured as transmission through high-finesse cavity, with calculated spectrum. (b) Modulator sensitivity from DC to 16 MHz, determined from height of sidebands in (a). (c) PDH error signal response to disturbance from 1.5 to 50 MHz. (d) Measured modulator sensitivity as the difference between measured PDH response and expected PDH response (points), with linear regression (dashed). The −3 dB bandwidth is 25 MHz.

changes to lock the laser frequency to a cavity resonance, and the high-frequency (FAST) output was connected to either the diode injection current or the intra-cavity modulator to reduce the laser linewidth. The laser was operated with an output power of 10 mW, and the power incident on the optical cavity was 150 μW.

Figure 4(b) (top) shows the cavity transmission and the PDH error signal when the laser is scanned through a cavity resonance. When the laser is locked to the resonance, the error signal reflects the feedback to maintain the laser at the transmission maximum [see Fig. 4(b) (bottom)].

In-loop noise spectra, measurements of the PDH error signal are shown in Fig. 5 for feedback to the intra-cavity modulator and to the diode injection current. The spectra were acquired with a 24-bit digitizer at 2.5×10^6 samples per second (up to 1 MHz) and an RF spectrum analyzer (above 1 MHz). The spectra were acquired with feedback off (unlocked, on resonance), with both piezo and fast feedback (full PID). The spectra were scaled from RF power to frequency noise density by using the slope of the error signal in Fig. 4(b).

For diode current feedback, a servo bump occurs at around 300 kHz, increasing to just above 1 MHz with maximum phase lead in the servo controller. For the intra-cavity modulator, the servo bump is found at up to 2.7 MHz, allowing greater gain and noise suppression; however, the maximum gain was limited by the onset of oscillation at a narrow resonance in the feedback loop at 1.8 MHz.

Finally, we performed an optical heterodyne (beat measurement) of the laser with a second ultra-stable light source. The laser was PDH locked to an ultra-high-finesse cavity (free spectral range 1.5 GHz, finesse 3×10^5, fractional frequency stability 2×10^{-15} at 1 s integration time) via a four-stage PI lock. Light was delivered from the cateye via optical fibers to both the cavity and a fast beat diode where it was overlapped with the second light source. The phase and amplitude noise from the fiber delivery were suppressed with additional PI stages and actuators to remove linewidth broadening effects. The reference source was a similarly stabilized Ti:sapphire laser with a linewidth of (1.7 ± 0.5) Hz determined by a three-cornered hat measurement with two similar systems co-located in Innsbruck (Austria). The absolute frequency difference between the two lasers leads to a beat signal centered around 86 MHz as recorded by a fast photodiode (Thorlabs PDA015A/M), with a central peak of (1.4 ± 0.1) Hz linewidth, as shown in Fig. 6(a). This linewidth is a convolution of the linewidths of the two sources and the resolution bandwidth of the spectrum analyzer (1 Hz) used to record the data, thus setting an upper bound on the true linewidth of 1 Hz. A more precise determination of the linewidth would require reference with even narrower linewidth or more complex self-homodyne techniques. When configured for minimum

10 November 2023 04:28:51

© Author(s) 2022

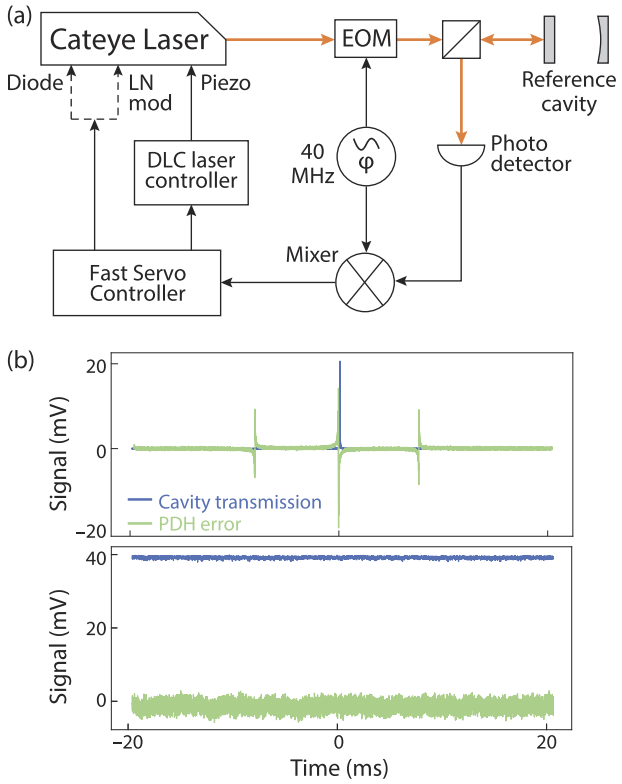

FIG. 4. (a) Simplified diagram of the Pound–Drever–Hall (PDH) locking setup, with the intracavity modulator inside a 729 nm wavelength cateye external cavity laser. (b) Cavity transmission and PDH error signals for laser scanning through the cavity resonance (top) and when locked (bottom).

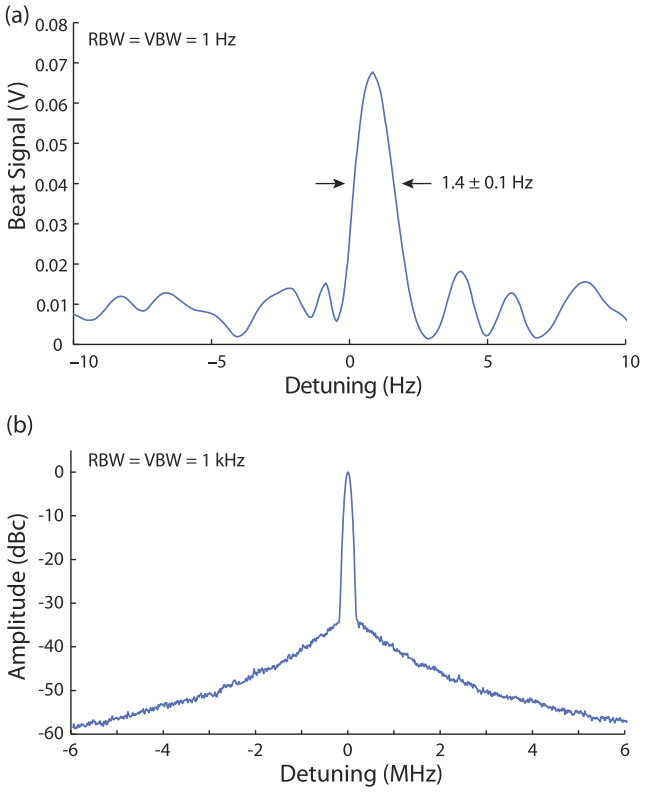

FIG. 6. (a) Beat signal between Ti:sapphire reference laser with the PDH-locked cateye laser, relative to the 86 MHz frequency difference between the two lasers. The linewidth of the resulting beat signal is a convolution of the linewidths of two sources and the spectrum analyzer (RBW 1 Hz), indicating an upper bound of 1 Hz for our laser linewidth. (b) Wide spectrum of the beat note, relative to 69 MHz, with lock parameters configured for a higher locking bandwidth.

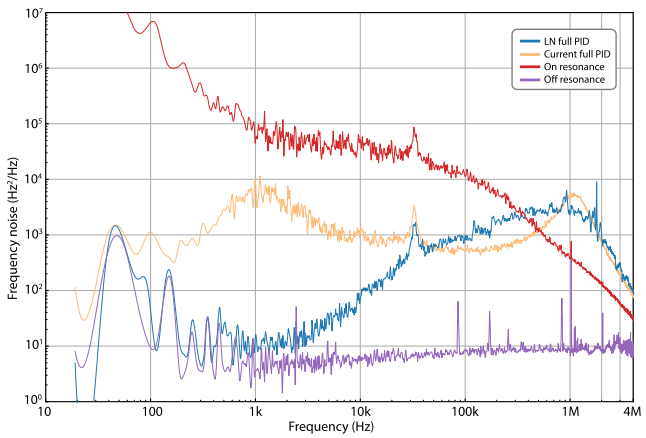

FIG. 5. In-loop noise spectra with feedback to intra-cavity modulator (LN full PID, blue) and to laser diode current (Current full PID, orange), compared to on resonance (no feedback) and off resonance.

linewidth, servo bumps appear at ±5 MHz but higher locking bandwidths up to 20 MHz were observed, at the expense of central feature linewidth [see Fig. 6(b)].

CONCLUSION

In conclusion, we have demonstrated that the cateye external cavity laser design lends itself to the incorporation of a fast electro-optic modulator based on an LN wafer. With an LN chip at the focus of the cateye, the electrodes can be closely spaced to achieve the frequency modulation needed for frequency stabilization and linewidth narrowing by using signals of a volt or less, compatible with standard analog electronics without high voltage drivers. The low voltage and small size and capacitance of the modulator allow high modulation bandwidth. We stabilized the laser to a high-finesse optical cavity with up to 1.8 MHz closed-loop bandwidth, achieving linewidth narrowing to 1 Hz. We expect that improved narrowing and higher bandwidth should be achievable, for example, by using a higher finesse cavity to improve the signal-to-noise ratio, and with faster electronics to reduce the closed loop group delay. The wafer design could be used more generally in laser cavities that incorporate a tight

10 November 2023 04:28:51

© Author(s) 2022

focus, for example, by placing the LN chip close to the emission facet of a laser diode in a Littrow or Littman–Metcalf configuration external cavity. We expect that when integrated into tunable lasers, the modulator will be useful for achieving high precision atomic clocks and high-fidelity rapid qubit operations with trapped ion quantum computers.

ACKNOWLEDGMENTS

The authors acknowledge the facilities, and the scientific and technical assistance, of the Micro Nano Research Facility (MNRF) and the Australian Microscopy and Microanalysis Research Facility at RMIT University. This work was performed, in part, at the Melbourne Centre for Nanofabrication (MCN) in the Victorian Node of the Australian National Fabrication Facility (ANFF). This research was supported by the ARC (Grant No. LP180100332). A.S., Ch.D.M., and T.M. acknowledge the support from the Austrian Science Fund (FWF), through SFB BeyondC (FWF Project No. F7109), and the IQI GmbH. T.M. and Ch.D.M. acknowledge funding from the Office of the Director of National Intelligence (ODNI), Intelligence Advanced Research Projects Activity (IARPA), via U.S. ARO Grant Nos. W911NF-16-1-0070 and W911NF-20-1-0007, and the U.S. Air Force Office of Scientific Research (AFOSR) via IOE Grant No. FA9550-19-1-7044 LASCEM.

AUTHOR DECLARATIONS

Conflict of Interest

Authors S.J.T.-W., N.L., P.M.F., and R.E.S. develop external cavity diode lasers at Moglabs.

Author Contributions

S. Palmer: Conceptualization (equal); Data curation (equal); Formal analysis (equal); Investigation (equal); Methodology (equal); Validation (equal); Writing – original draft (equal); Writing – review & editing (equal). **A. Boes**: Formal analysis (supporting); Supervision (equal); Validation (supporting); Writing – review & editing (equal). **G. Ren**: Formal analysis (supporting); Supervision (supporting); Validation (supporting); Writing – review & editing (equal). **T. G. Nguyen**: Formal analysis (supporting); Supervision (equal); Validation (supporting); Writing – review & editing (equal). **S. J. Tempone-Wiltshire**: Data curation (equal); Investigation (equal); Methodology (equal); Resources (supporting); Validation (supporting). **N. Longhurst**: Data curation (equal); Investigation (equal); Methodology (equal); Resources (supporting); Validation (supporting). **P. M. Farrell**: Data curation (equal); Investigation (equal); Methodology (equal); Resources (supporting); Validation (supporting). **A. Steiner**: Data curation (supporting); Formal analysis (supporting); Investigation (supporting); Validation (supporting); (supporting). **Ch. D. Marciniak**: Data curation (supporting); Formal analysis (supporting); Supervision (supporting); Validation (supporting); Writing – review & editing (supporting). **T. Monz**: Data curation (supporting); Formal analysis (supporting); Supervision (supporting); Validation (supporting). **A. Mitchell**: Formal analysis (supporting); Funding acquisition (lead); Resources (equal); Supervision (equal); Validation (equal); Writing – review & editing (equal). **R. E. Scholten**: Conceptualization (equal); Data curation (equal); Formal analysis (equal); Funding acquisition (supporting); Investigation (equal); Methodology (equal); Resources (equal); Supervision (equal); Validation (equal);.

DATA AVAILABILITY

The data that support the findings of this study are available from the corresponding author upon reasonable request.

REFERENCES

[1] L. Gianfrani, R. W. Fox, and L. Hollberg, "Cavity-enhanced absorption spectroscopy of molecular oxygen," J. Opt. Soc. Am. B **16**(12), 2247–2254 (1999).
[2] A. Cabral and J. Rebordao, "Accuracy of frequency-sweeping interferometry for absolute distance metrology," Opt. Eng. **46**(7), 073602 (2007).
[3] Y. Y. Jiang *et al.*, "Making optical atomic clocks more stable with 10^{-16}-level laser stabilization," Nat. Photonics **5**(3), 158–161 (2011).
[4] T. W. Hänsch and A. L. Schawlow, "Cooling of gases by laser radiation," Opt. Commun. **13**(1), 68–69 (1975).
[5] J. I. Cirac and P. Zoller, "Quantum computations with cold trapped ions," Phys. Rev. Lett. **74**(20), 4091–4094 (1995).
[6] S. L. Campbell *et al.*, "A Fermi-degenerate three-dimensional optical lattice clock," Science **358**(6359), 90–94 (2017).
[7] G. E. Marti, R. B. Hutson, A. Goban, S. L. Campbell, N. Poli, and J. Ye, "Imaging optical frequencies with 100 μHz precision and 1.1 μm resolution," Phys. Rev. Lett. **120**(10), 103201 (2018).
[8] J. P. McGilligan, P. F. Griffin, R. Elvin, S. J. Ingleby, E. Riis, and A. S. Arnold, "Grating chips for quantum technologies," Sci. Rep. **7**(1), 384 (2017).
[9] N. Akerman, N. Navon, S. Kotler, Y. Glickman, and R. Ozeri, "Universal gate-set for trapped-ion qubits using a narrow linewidth diode laser," New J. Phys. **17**(11), 113060 (2015).
[10] C. E. Wieman and L. Hollberg, "Using diode lasers for atomic physics," Rev. Sci. Instrum. **62**(1), 1–20 (1991).
[11] B. C. Young, F. C. Cruz, W. M. Itano, and J. C. Bergquist, "Visible lasers with subhertz linewidths," Phys. Rev. Lett. **82**(19), 3799–3802 (1999).
[12] H. Stoehr, F. Mensing, J. Helmcke, and U. Sterr, "Diode laser with 1 Hz linewidth," Opt. Lett. **31**(6), 736–738 (2006).
[13] A. D. Ludlow *et al.*, "Compact, thermal-noise-limited optical cavity for diode laser stabilization at 1×10^{-15}," Opt. Lett. **32**(6), 641–643 (2007).
[14] A. Celikov *et al.*, "External cavity diode laser high resolution spectroscopy of the Ca and Sr intercombination lines for the development of a transportable frequency/length standard," in *Proceedings of the 1995 IEEE International Frequency Control Symposium (49th Annual Symposium)* (IEEE, 1995), pp. 153–160.
[15] J. Le Gouët, J. Kim, C. Bourassin-Bouchet, M. Lours, A. Landragin, and F. Pereira Dos Santos, "Wide bandwidth phase-locked diode laser with an intra-cavity electro-optic modulator," Opt. Commun. **282**(5), 977–980 (2009).
[16] N. Beverini, E. Maccioni, P. Marsili, A. Ruffini, and F. Sorrentino, "Frequency stabilization of a diode laser on the Cs D_2 resonance line by the Zeeman effect in a vapor cell," Appl. Phys. B **73**(2), 133–138 (2001).
[17] D. J. Thompson and R. E. Scholten, "Narrow linewidth tunable external cavity diode laser using wide bandwidth filter," Rev. Sci. Instrum. **83**(2), 023107 (2012).
[18] R. W. Fox, C. W. Oates, and L. W. Hollberg, "1. Stabilizing diode lasers to high-finesse cavities," Exp. Methods Phys. Sci. **40**, 1–46 (2003).
[19] R. W. P. Drever *et al.*, "Laser phase and frequency stabilization using an optical resonator," Appl. Phys. B: Photophys. Laser Chem. **31**(2), 97–105 (1983).

10 November 2023 04:28:51

© Author(s) 2022